

The synergistic effect of poly(acrylamide-co-4-vinylpyridine) copolymer "AM-4VP-24" and iodide ion on corrosion inhibition of mild steel in 1M H₂SO₄

Ali Mansri ^{a,*} and Brahim Bouras ^a

^a Laboratoire d'Application des Electrolytes et des Polyélectrolytes Organiques (LAEPO). Université de Tlemcen. Département de Chimie. B. P. 119 13000 Tlemcen, Algeria

*Corresponding Author: Email address: a_mansri@mail.univ-tlemcen.dz,
bourasbrahim_m8@yahoo.fr Tel./Fax: 00 213 43286308

Received 08 July 2014, Revised 20 September 2014, Accepted 28 September 2014.

Abstract

The effect of iodide ions on the corrosion inhibition of mild steel in 1 M sulfuric acid in the presence of poly(acrylamide-co-4-vinylpyridine) copolymer abbreviated by (AM-4VP-24) newly synthesized has been investigated by weight loss measurements and electrochemical techniques (polarization curves and impedance spectroscopy) at 18°C. The obtained results showed that the inhibition efficiency increased with increasing copolymer concentration. It was also found that inhibition efficiency increased with addition of potassium iodide (KI) to the copolymer. A synergistic effect was observed between the copolymer and KI. On the other hand, it was found that the inhibiting effect of the system (copolymer + KI) increased with increasing immersion time. The inhibitor was adsorbed on the steel surface according to the Langmuir adsorption isotherm model.

1. Introduction

An important practical application of such phenomena is corrosion inhibition and numerous investigations have been performed on the inhibition of steel, iron, and iron-based alloy by using of organic compounds [1-10]. Most of the well-known organic acid inhibitors contained nitrogen, sulfur and oxygen [11-15]. The results show that the inhibitory efficiency increases with inhibitor concentrations. Therefore, they minimize the direct interaction between the metal and corrosive agents. In some cases, the coordination of the inhibitor molecules to the surface is weak, and their presence in the corrosive solutions required maintaining the desired concentration of these agents to the metal surface [15-24].

For polymer inhibitors, Polymer amines have been found to be efficient corrosion inhibitors for iron in acidic solutions because of the presence of abundance of π -electrons and unshared electrons pairs on nitrogen atom which can interact with the empty d-orbital of iron [25].

Polyacrylamide [26, 27], polyacrylic acid [28], poly(4-vinylpyridine) [29], poly(4-vinylpyridine isopentyl bromide) [30] and poly(4-vinylpyridine poly-3-oxide ethylene) [31] have been reported as efficient corrosion inhibitors for iron in acidic media.

Some authors have reported synergistic inhibition between halide ions and some compounds including polymers. Earlier studies have shown that halide ions synergistically increased the corrosion inhibition efficiency of polyethylene glycol, polyvinyl alcohol, polyacrylamide, polyvinyl pyrrolidone and poly(4-vinylpyridine) for mild steel in acidic media [26, 32–36].

Concerning the effect of the copolymer as the corrosion when de 4VP was introduced in the copolymer, the influence of halide ions on the corrosion inhibition of metals by AM-co-4VP copolymer has been investigated by Mansri and al [37].

In this work, we have synthesized another new copolymer which contains high percentage of 4VP. In the order to quantify the inhibition efficiency and to evaluate the synergistic effect with I^- ions of this copolymer, the gravimetric and electrochemical measurements were made using mild steel immersed in molar sulphuric acid without and with addition of acrylamide and 4-vinylpyridine copolymer in absence and in presence of iodide ions.

2. Methods and materials

2.1. Synthesis and characterise of the copolymer

The acrylamide compound was provided from Merck. 4VP (Aldrich, 98%) was dried over calcium hydride overnight and fractionally distilled under reduced pressure (68°C- 69°C at 15mmHg), having discarded the first and last 10% of the monomer. Ammonium persulfate (Aldrich) was used as initiator without further purification.

The poly(acrylamide-co-4-vinylpyridine) copolymer "AM-4VP-24" was obtained with a yield 90% and prepared by radical polymerization of acrylamide (AM) and 4-vinylpyridine (4VP) in aqueous solution, with ammonium persulfate (APS) as initiating agent. The copolymer was repeatedly precipitated in ethanol. The product was then dried under vacuum at room temperature to constant weight and stored in a desiccator.

The molecular structure of newly synthesised copolymer is shown in Figure 1.

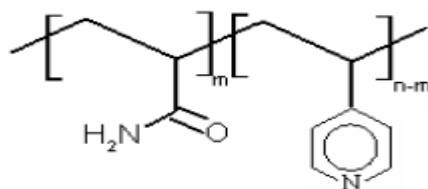


Figure 1. Chemical structure of the poly(acrylamide-co-4-vinylpyridine) copolymer

It was also purified via several cycles of solubilisation/precipitation in the following couple of solvent/non-solvent (water/ethanol). The product obtained is a pure powder. The copolymer

was characterised by proton nuclear magnetic resonance (^1H NMR) spectra with a DMX-500 (Bruker, Germany) and the solvents were $\text{D}_2\text{O}/\text{DCI}$.

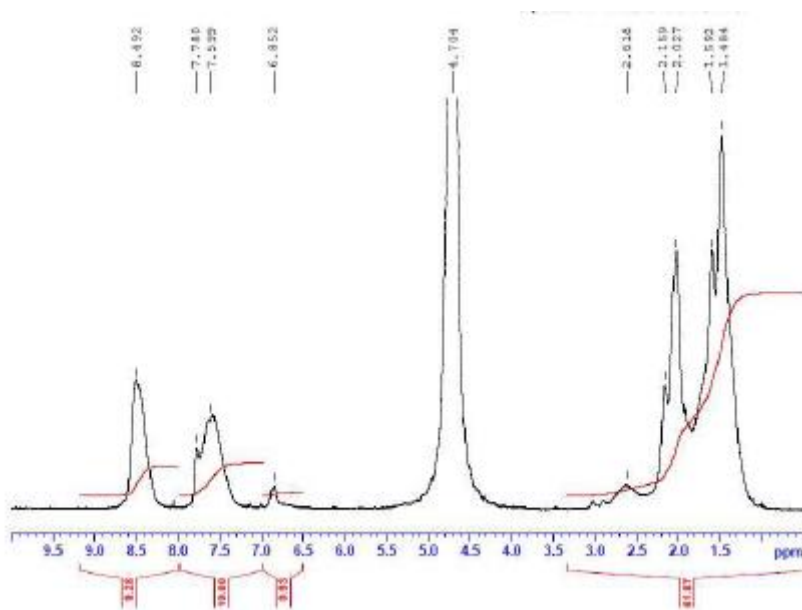


Figure 2. ^1H NMR spectra of poly(acrylamide-co-4-vinylpyridine) copolymer in $\text{D}_2\text{O}/\text{DCI}$

The ^1H NMR spectra of poly(acrylamide-co-4-vinylpyridine) copolymer is shown in Figure 2, with the following spectral data:

- 1.48-1.59 ppm ($-\text{CH}_2-$) of the linear chains of the copolymer [37-40]
- 2.03-2.16 ppm ($-\text{CH}-$) of the linear chains of the copolymer [37-40]
- 4.7 ppm (solvent protons)
- 6.85 ppm (H atom at ortho position of N of 4VP).
- 7.60-7.78 ppm (H atom at the meta position of N and the ortho position of N^+ of 4VP).
- 8.49 ppm (H atom at the meta position of N^+ of 4VP) [37, 39-41].

The UV-visible absorption spectra (Figure 3) were recorded with a Shimadzu UV 260 spectrophotometer. The presence of the 4VP in the poly(acrylamide-co-4-vinylpyridine) copolymer is confirmed by UV-visible spectrum. The monomer of the 4VP shows an intense absorption at 205 nm which is connected to the $n-\pi^*$ and at 256 nm which is connected to the $\pi-\pi^*$ bands. This result is in agreement with the results of Bernard et al. [42]. However, the acrylamide monomer does not show any absorption in this area. From the ^1H NMR and UV-visible spectra, we calculated the percentage (%) of 4VP and acrylamide in the copolymer chains.

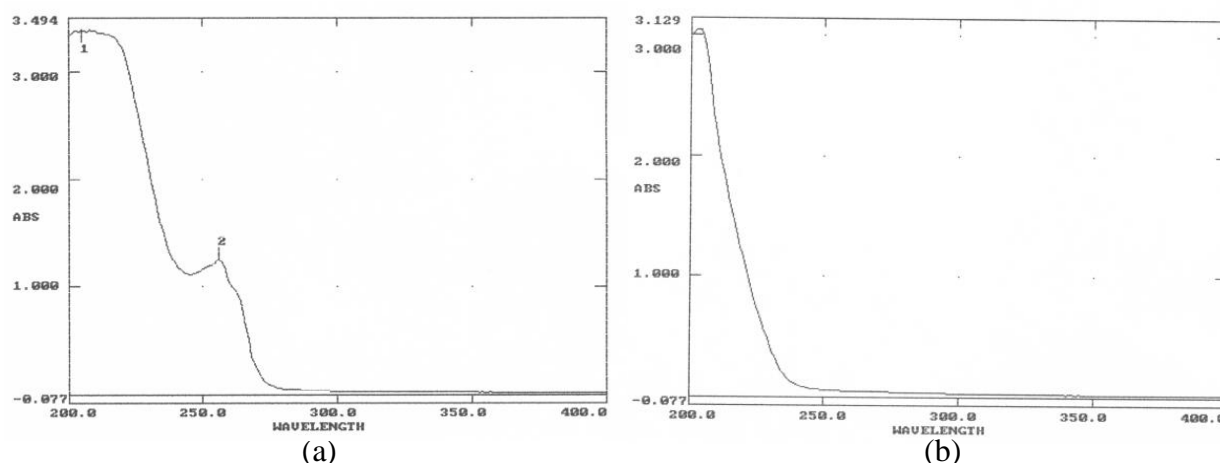


Figure 3. UV-visible spectra in aqueous solution at ambient temperature
 a) of poly(acrylamide-co-4-vinylpyridine) copolymer b) of polyacrilamide polymer

Table 1. gives the values of weight rapport of acrylamide and 4-vinylpyridine monomers in the copolymer obtained from the ^1H NMR and UV-visible spectra.

Table 1. ^1H NMR and UV-visible results

Copolymer	Conversion rate %	w/w% of AM/4VP with ^1H NMR final	w/w% of AM/4VP with UV –visible final
poly(acrylamide-co-4-vinylpyridine)	90	75.6 / 24.4	75.9 / 24.1

The molecular weight was determined by water size exclusion chromatography (GPC) using a set of three columns TSK PWXL obtained from TOSO Haas (length $\frac{1}{4}$ 30 cm, interior diameter $\frac{1}{4}$ 7.8 cm) and coupled to an automatic refract-meter or light scattering apparatus, and the molecular weight was also determined by a capillary standard Ubbelohde viscometer, with a thermostated bath at $25 \pm 0.1^\circ\text{C}$.

Table 2. gives the results of the poly(acrylamide-co-4-vinylpyridine) copolymer obtained by water size exclusion chromatography (GPC) and viscosimetry

Table 2. GPC and viscosity results

Copolymer	M_v (g/mole)	M_w (GPC) (g/mole)	M_n (GPC) (g/mole)	I_p
poly(acrylamide-co-4-vinylpyridine)	1.4×10^5	2.6×10^5	8.5×10^4	3

2.2. Samples and materials

Prior to each gravimetric or electrochemical experiment, the surface of the specimens was abraded successively with emery paper. The samples were polished finally with emery paper up 1200 grade. Weight loss was measured on sheets of steel of 2 cm^2 apparent surface area. The specimens were then rinsed with acetone and bi-distilled water before being weighed and immersed in 50 ml of the corrosive medium. A clean weighed mild steel sample was

completely immersed at an inclined position in the vessel for 4 h of immersion in 1 M H₂SO₄, with and without the addition of inhibitor at different concentrations.

A solution of 1 M H₂SO₄ was prepared from an analytical reagent grade 98 % H₂SO₄ and bi-distilled water and was used as corrosion media. The chemical composition of mild steel is given in Table 3.

Table 3. The chemical composition of mild steel

%C	%Si	%Mn	%S	%Al	%Cu	%Fe
0.14	0.21	0.09	0.012	0.01	0.006	Balance

Electrochemical measurements were carried out in a conventional three-electrode electrolysis cylindrical Pyrex glass cell. The working electrode had the form of a disc cut from iron sheet. The exposed area to the corrosive solution was 1 cm². A saturated calomel electrode (SCE) and a platinum electrode were used, respectively as a reference and auxiliary electrodes. All potentials are given in the SCE scale. The cell is thermostated at 291 ± 1 K.

The current–voltage curves are recorded with a potentiostat (Amel 549) using a linear sweep generator (Amel 567) at a scan rate of 1 V/min. Before recording the cathodic curves, the iron electrode was polarised at 800 mV for 10 min. For anodic curves, the potential of the electrode was swept from its open circuit value after 30 min free corrosion. The test solution was de-aerated for 30 min in the cell with pure nitrogen. Gas bubbling was maintained throughout the experiments.

Electrochemical impedance spectroscopy (EIS) was carried out with a voltalab PGZ 100 electrochemical system at E_{corr} after immersion in solution. After determination of the steady-state current at a given potential, sine wave voltage (10 mV) peak to peak, at frequencies between 100 kHz and 10 mHz, was superimposed on the rest potential. Computer programs automatically controls the measurements performed at rest potentials after 30 min of exposure. EIS diagrams are given in the Nyquist representation.

3. Results and discussion

3.1. Weight loss measurements

3.1.1. Concentration effect of the poly(acrylamide-co-4-vinylpyridine) copolymer

The effect of addition of the copolymer tested at different concentrations on the corrosion of steel in 1M H₂SO₄ solution was studied by weight loss at 18 °C after 4 h of immersion. Inhibition efficiency (E_w %) was calculated using Eq. (1):

$$E_w = \left(1 - \frac{W_{corr}}{W_{corr}^o}\right) \times 100 \quad (1)$$

Where W_{corr} and W_{corr}^o are the corrosion rates of steel in the presence and absence of the inhibitor, respectively.

Table 4. Inhibition efficiency for corrosion of mild steel in 1M H₂SO₄ with different concentrations obtained from weight loss measurements at 18°C.

C(copolymer) (mg l ⁻¹)	W _{corr} (mg cm ⁻² h ⁻¹)	E _w (%)
Blank	0.1686	—
10 ⁻¹	0.0773	54.17
1	0.0686	59.30
5	0.0634	62.40
10	0.0570	66.20

Table 4. gives the values of inhibition efficiency obtained from the weight loss measurements for different concentrations of copolymer in 1 M H₂SO₄. The results show that the inhibition efficiency increases with increasing inhibitor concentrations. The inhibition by the copolymer can be explained in terms of adsorption on the metal surface. The adsorption of the copolymer molecules could occur due to the formation of links between the d-orbital of iron atoms, involving the displacement of water molecules from the metal surface, and the lone electron pairs.

It is shown that the compounds, having a higher electron density load around the heteroatoms specially nitrogen atoms, exhibit protective properties which depend upon their ability to reduce the corrosion rate. Effectively, the heterocyclic-containing nitrogen in the polymer structure and electronegative functional groups, π electrons and the conjugated double bands have been proved to perform as inhibitors of the corrosion [15, 34, 35, 43, 44]. The compound can be absorbed by the interaction between the lone pair of electrons of the nitrogen and oxygen atoms and the metal surface. The optimum concentration required to achieve an efficiency of 66.20 % is found to be 10 mg l⁻¹.

3.1.2. Synergic effect

The results of the inhibition efficiency for the corrosion of mild steel in 1M H₂SO₄ in the presence of 10 and 10⁻¹ mg l⁻¹ of the copolymer with different concentrations of KI obtained from weight loss measurements at 18°C after 4h immersion are listed in Table 5.

Figure 4. shows a clear increase in inhibition efficiencies according to the concentration of the KI. This result indicates the synergetic effect between the copolymer and KI. The maximum of synergy is observed for a precise concentration of KI for each case. Any later increase in the concentration of KI is accompanied by a reduction in the value of the inhibition efficiency. These results are in agreement with the literature [27, 33]. For the high concentration of copolymer (C_P = 10 mg/l), we observe, first an increase in the synergy effect which reaches a maximum (E (%) = 90.37 %) for a weak concentration of the KI (0.01 %). Beyond this value, by increasing the KI concentration, the value of the inhibition efficiency decreases. For the low concentration of copolymer (C_P = 10⁻¹ mg/l), we observe an increase in the synergy effect

according to the KI concentration and the value of the inhibition efficiency attains the maximal value 89.26 % at 0.015 % of KI concentration. After this value, we observe a decrease in this synergy effect, which reached 82.54 % for a concentration of KI (0.018 %). We note, the maximum of synergy is reached for a concentration of KI which is high compared to the first case. The results obtained in Table 5. are represented in Figure 4.

Table 5. Inhibition efficiency for different concentrations of KI of mild steel in 1M H₂SO₄ in presence of 10 and 10⁻¹ mg l⁻¹ of the poly(acrylamide-co-4-vinylpyridine) copolymer

C(copolymer) (mg l ⁻¹)	C(KI) (%)	W _{corr} (mg cm ⁻² h ⁻¹)	E _w (%)
10	0	0.0570	66.20
	0.005	0.0210	87.54
	0.010	0.0162	90.37
	0.015	0.0213	87.36
10 ⁻¹	0	0.0773	54.17
	0.005	0.0274	83.75
	0.010	0.0228	86.47
	0.015	0.0181	89.26
	0.018	0.0294	82.54

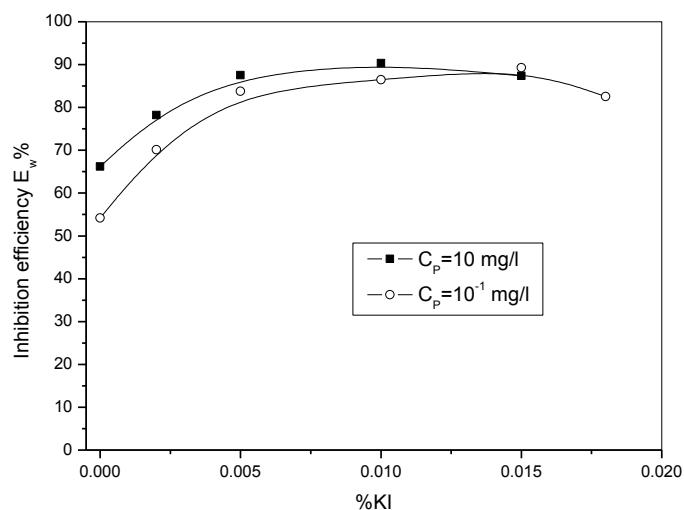


Figure 4. Variation of inhibition efficiency of mild steel in 1M H₂SO₄ in the presence of the copolymer for various concentrations according to the KI concentration at 18°C

3.1.3. Effect of immersion time

The results obtained of the inhibition efficiency for the corrosion of mild steel in 1 M H₂SO₄ with 10⁻¹ and 10 mg l⁻¹ of poly(acrylamide-co-4-vinylpyridine) copolymer in the presence of 0.01 % KI obtained from weight loss measurements at 18 °C after different times of

immersion are listed in Table 6. The results show that there is an increase in the Inhibition efficiency with an increasing time of immersion which is in agreement with the literature [32]. So we note that the increases in the Inhibition efficiency was more pronounced for the high concentration of copolymer compared to the weak concentration.

Table 6. Inhibition efficiency for 0.01% of KI of mild steel in 1M H₂SO₄ in presence of poly(acrylamide-co-4-vinylpyridine) copolymer at different concentrations

C(copolymer) (mg l ⁻¹)	Immersion time (h)	W _{corr} (mg cm ⁻² h ⁻¹)	E _w (%)
10	4	0.0162	90.37
	8	0.0121	92.85
	12	0.0110	93.46
	24	0.0090	94.65
10 ⁻¹	4	0.0228	86.47
	8	0.0213	87.35
	12	0.0211	87.47
	24	0.0203	87.98

3.2. Polarisation measurements

3.2.1. Concentration effect of the poly(acrylamide-co-4-vinylpyridine) copolymer

Current–potential characteristics resulting from cathodic and anodic polarization curves of steel in 1 M H₂SO₄ in presence of the copolymer at various concentrations are evaluated. The cathodic Tafel plots of the copolymer are shown in Figure 5. Table 7 shows electrochemical parameters and inhibition efficiencies (E_i) are determined by Eq. (2):

$$E_i \% = \left(1 - \frac{I_{corr}}{I_{corr}^0}\right) \times 100 \quad (2)$$

where I_{corr} and I_{corr}⁰ are the corrosion current density values with and without the inhibitor, respectively, determined by extrapolation of cathodic Tafel lines to the corrosion potential.

The polarisation resistance (R_p) and corresponding efficiency inhibition values of mild steel in 1 M H₂SO₄ in the absence and presence of different concentration of the inhibitor are also given in Table 7. In this case the inhibition efficiency (E_R%) is calculated by Eq. (3):

$$E_R \% = \frac{R'_p - R_p}{R'_p} \times 100 \quad (3)$$

where R_p and R'_p are the polarisation resistance with and without the inhibitor, respectively.

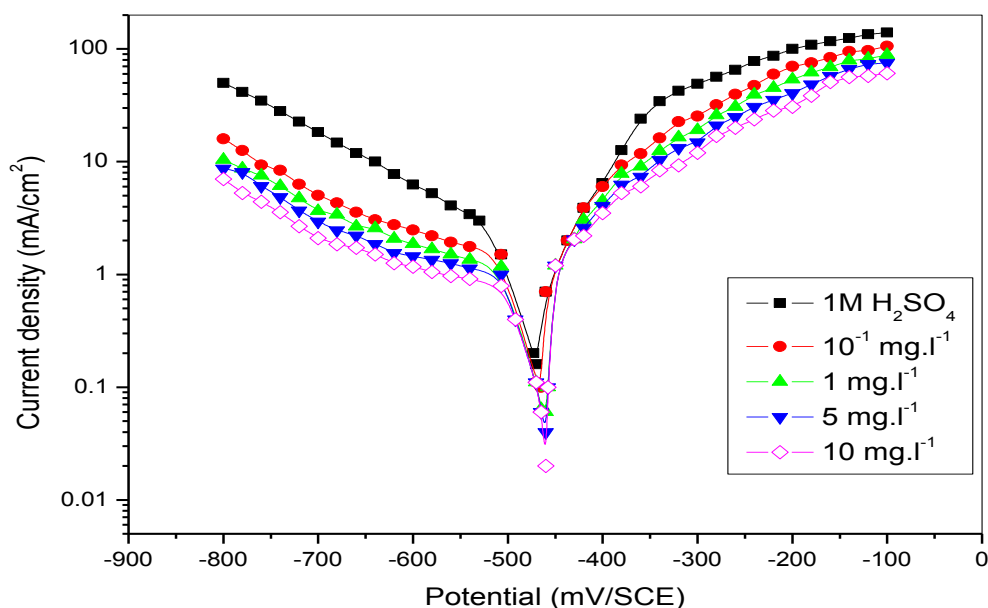


Figure 5. Potentiodynamic polarization curves for mild steel in 1 M H_2SO_4 containing different concentrations of poly(acrylamide-co-4-vinylpyridine) copolymer.

The increase in the copolymer concentrations causes a decrease in the corrosion rate, that is, shifts both the anodic and cathodic curves and to lower values of current densities. This implies that the hydrogen evolution reactions are inhibited. This may be ascribed to adsorption of the copolymer over the corroding surface [27, 32, 45]. From results obtained in Table 7, we note a decrease of corrosion current densities when the increase of the concentration of the inhibitor. The inhibiting action is more pronounced with an inhibitor and their inhibition efficiency attains a maximum value of 68.14 % at 10 mg/L. It is also observed that the presence of the copolymer does not shift E_{corr} remarkably, the values remain almost unchanged.

The parallel Tafel curves obtained indicate that hydrogen evolution reactions are activation-controlled and the addition of the copolymer does not modify the mechanism of this process [7, 15]. The anodic curves, with and without the copolymer inhibitor, show that the inhibition mode depended upon the electrode potential. In the case where the corrosion inhibition depends on the potential of the electrode, the observed phenomena are generally described as corrosion inhibition of the interface associated with the formation of a protective layer of adsorbed inhibition species at the electrode surface [27–30].

Being weakly basic, the inhibitor, rapidly protonated in acid solutions exists in their cationic form. Due to electrostatic attraction, the inhibitors are strongly adsorbed onto the electron-rich areas blocking the cathodic sites. This is in agreement with the increase of the cathodic overpotential and shift of the steady corrosion potential to less noble direction in presence of inhibitors. Effectively, the heterocyclic-containing nitrogen in the polymer structure and

electronegative functional groups, π electrons and the conjugated double bands have been proved to perform as very good inhibitors for the corrosion of pure iron in acidic solution [6,7, 15, 21, 46]. We conclude that the copolymer has an effect on the cathodic and anodic behaviour of steel and that the compound acts as a mixed inhibitor.

From polarisation resistance measurements (Table 7), we remark that R_p increases with increasing of copolymer inhibitor concentration. $E\%$ increases with the increase of inhibitor concentration to attain 65.85 % at 10 mg l^{-1} . We may conclude that the inhibition efficiencies of the copolymer obtained by electrochemical, polarisation resistance and weight loss methods are in good agreement.

Table 7. Corrosion data of mild steel in 1 M H_2SO_4 with and without the copolymer at 18°C

C (mg l ⁻¹)	E _{corr} (mV/SCE)	b _c (mV/dec)	I _{corr} (μA/cm)	E _i (%)	R _p (Ω cm ²)	E _R (%)
0	-465	235	1650	—	22	—
10 ⁻¹	-461	245	723	56.20	47	53.03
1	-460	253	636	61.55	54	59.13
5	-460	243	600	63.64	57	61.57
10	-461	248	526	68.14	64	65.85

3.2.2. Effect of iodide ion

Halide ions are known to improve the adsorption of some organic cations type inhibitors on corroding metal surface thereby enhancing its inhibition efficiency considerably. This phenomenon, which has been ascribed to as synergistic effect is often most pronounced with iodide ions.

Experiments were undertaken in this present study to assess the effect of addition of iodide ions on the corrosion inhibition performance of the copolymer for mild steel in 1 M H_2SO_4 . Figure 6. shows the potentiodynamic polarization curves in the absence and presence of different concentrations of iodide ion at 18°C .

It is clear from the figure that the addition of the iodide ions shifts the E_{corr} to positive values and reduced both the anodic iron dissolution and cathodic hydrogen evolution reactions. The i_{corr} were reduced in the presence of the iodide ions compared to their absence. The values of i_{corr} depend to iodide concentration. Similar observation has been reported in the literature [27, 33, 47].

The addition of iodide ions to the copolymer produces pronounced effects on the anodic and cathodic currents compared to those obtained in the presence of just the copolymer, but in the cathodic current was more significant than that of the anodic current.

The electrochemical parameter obtained from the polarization curves are listed in Table 8. The results indicate that the corrosion current density is reduced from $1650 \mu\text{A cm}^{-2}$ in the free acid solution to $526 \mu\text{A cm}^{-2}$ in the presence of the copolymer. These values were further reduced to $122 \mu\text{A cm}^{-2}$ after the introduction of different concentrations of KI.

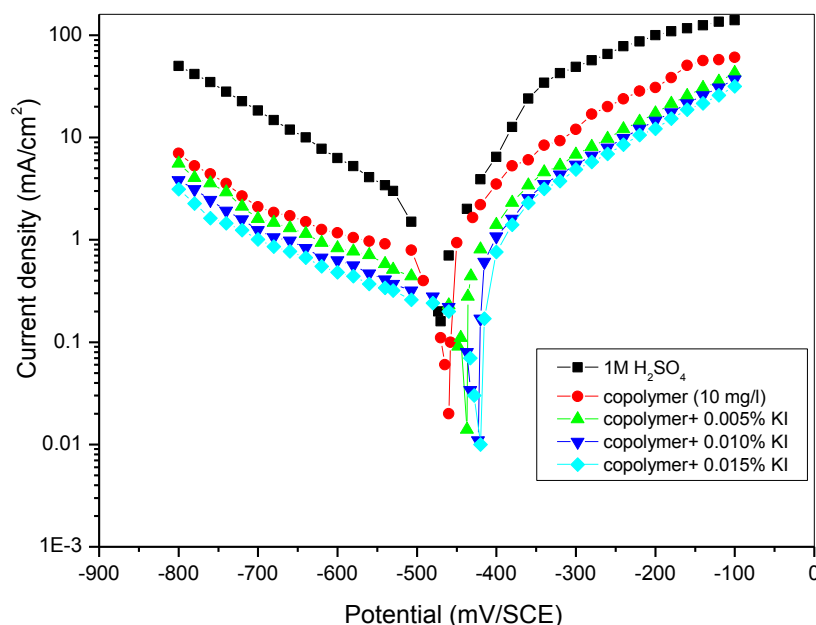


Figure 6. Potentiodynamic polarization curves for mild steel in 1 M H₂SO₄ in presence 10 mg l⁻¹ of the copolymer containing different concentrations of KI at 18°C

It is clearly seen that the combination of the copolymer and KI decreased considerably the corrosion current densities compared to the free acid and the copolymer solutions leading to higher inhibition efficiency. This is a clear indication of synergistic effect between the copolymer and KI.

Table 8. Potentiodynamic polarisation parameters for corrosion of mild steel in 1 M H₂SO₄ in presence 10 mg l⁻¹ of the copolymer containing different concentrations of KI at 18°C

C (KI) %	E _{corr} (mV/SCE)	b _c (mV/dec)	I _{corr} (μA/cm)	E _I (%)	R _P (Ω cm ²)	E _R (%)
Blank	-465	235	1650	—	22	—
0	-461	248	526	68.14	64	65.85
0.005	-440	270	170	89.70	156	85.92
0.010	-423	238	122	92.60	222	90.10
0.015	-420	237	174	89.45	164	86.60

3.3. Impedance measurements

3.3.1. Concentration effect of the poly(acrylamide-co-4-vinylpyridine) copolymer

To complete and to compare the results obtained previously, the corrosion behaviour of mild steel, in sulfuric acid solution with and without inhibitors, was investigated by EIS at 291 K. The corrosion behaviour of mild steel in 1M H₂SO₄ in the presence and absence of the copolymer is also investigated by the electrochemical impedance spectroscopy (EIS) at 291 K after 30 min of immersion (Figure 7). The charge-transfer resistance (R_t) values were

calculated from the difference in impedance at lower and higher frequencies [11, 26]. The double layer capacitance (C_{dl}) was obtained at the frequency f_m at which the imaginary component of the impedance is maximal ($Z_{i,max}$) by Eq. (4):

$$C_{dl} = \frac{1}{2\pi f_m \cdot R_t} \quad (4)$$

The inhibition efficiency from the charge transfer- resistance was calculated by Eq. (5):

$$E_{R_t} (\%) = \frac{R'_t - R_t}{R'_t} \times 100 \quad (5)$$

where R_t and R'_t are the charge transfer-resistance values with and without the inhibitor, respectively.

Typical Nyquist diagrams obtained in the presence of various concentrations of the copolymer are shown in Figure 7. The deduced impedance parameters as transfer resistance R_t ($\Omega \text{ cm}^2$), double-layer capacitance C_{dl} ($\mu\text{F}/\text{cm}^2$) and corresponding inhibition efficiency ($E_{R_t} \%$) are shown in Table 9. It is seen from Figure 7 that the impedance diagrams show semi-circles. We remark that the increase of R_t and decrease of double-layer capacitance (C_{dl}) and the efficiency increases when the concentration of the copolymer increases.

The obtained impedance diagrams show almost a semi-circular appearance, indicating a charge transfer process mainly controls the corrosion of mild steel. In fact, the presence of copolymer compound enhances the value of R_t in acidic solution.

Values of double-layer capacitance are also brought down to the maximum extent in the presence of the copolymer and the decrease in the values of C_{dl} follows the order similar to that obtained for I_{corr} in this study. The decrease in C_{dl} may be due to the adsorption of this compound on the metal surface, leading to the formation of film from acidic solution [17, 27, 30, 32, 48].

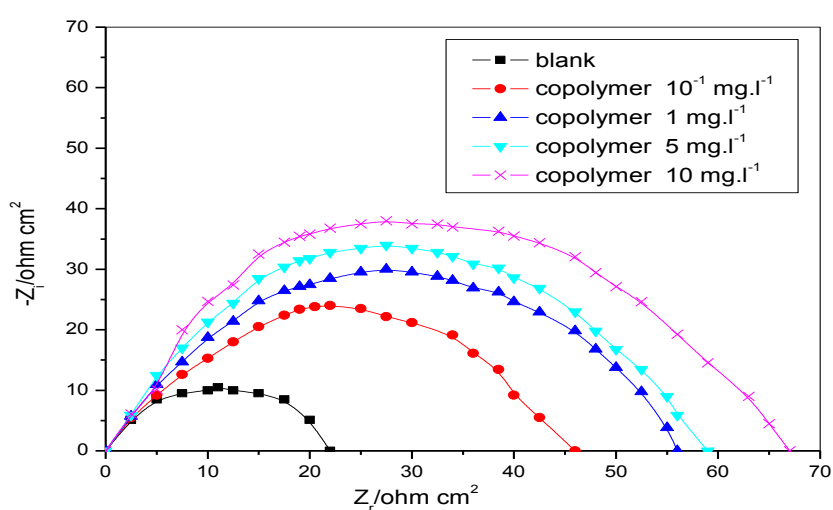


Figure 7. Nyquist plots for mild steel in 1 M H_2SO_4 containing different concentrations of poly(acrylamide-co-4-vinylpyridine) copolymer

Table 9. Impedance parameters for corrosion of mild steel in 1 M H₂SO₄ with different concentrations of poly(acrylamide-co-4-vinylpyridine) copolymer

C (copolymer) mg l ⁻¹	R _t (Ω cm ²)	C _{dl} (μF cm ⁻²)	E(%)
Blank	22	93	—
10 ⁻¹	46	47	52.40
1	56	37	60.54
5	59	35	62.75
10	67	30	67.10

3.3.2. Effect of iodide ion

In order to assess the effect of iodide ions additive on the corrosion inhibition of the copolymer for mild steel in 1 M H₂SO₄, electrochemical impedance spectroscopy measurements were undertaken using a fixed concentration of the copolymer (10 mg l⁻¹) combined with different concentrations of KI (0.005–0.015 %). The Nyquist plots in this case are similar of their homologue in absence of KI. So we note that, the results clearly show a distinct effect of the iodide ions additive on the corrosion behaviour of steel compared to the blank acid solution in the absence and the presence of the copolymer alone. In comparison with the copolymer alone, the size of the semicircle in Nyquist plot increases with all increase on the addition of iodide ions to copolymer. The addition of the iodide ions further enhances R_t values and reduces C_{dl} values. This can be attributed to the enhanced adsorption of the copolymer in the presence of KI because of the synergistic effect of iodide ions.

The impedance parameters derived from these investigations are mentioned in Table 10. As we notice, the results shows that addition of iodide ions to 10 mg l⁻¹ of the copolymer increased the charge transfer-resistance values from 22 Ω cm² in the free acid solution to 67 Ω cm² in the presence of the copolymer. These values increased further to 321 Ω cm² on the introduction of different concentrations of KI. Inhibition efficiency was also found to be upgraded from 67.10 % in the presence of 10 mg l⁻¹ of the copolymer to 91.15 % on addition of varying concentrations of KI to 10 mg l⁻¹ of the copolymer solution. The improved inhibition efficiency caused by the addition of iodide ions to the copolymer was due to synergistic effect between the copolymer and KI.

Table 10. Impedance parameters for corrosion of mild steel in 1 M H₂SO₄ in presence 10mg l⁻¹ of the copolymer in the absence and presence of various concentration of KI at 18°C

C(KI) %	R _t (Ω cm ²)	C _{dl} (μF cm ⁻²)	E(%)
Blank	22	93	—
0	67	30	67.10
0.005	134	15	83.65
0.010	287	07	92.35
0.015	321	06	93.15

3.4. Time effect

The addition of KI further enhances R_t values. This can be attributed to the enhanced adsorption of the copolymer in the presence of KI because of the synergistic effect of the iodide ions. Nyquist plots for mild steel in 1 M H_2SO_4 in the presence of 10 mg/l of the copolymer in combination with 0.010 % KI for different immersion times are shown in Figure 8. The Nyquist plots were recorded after different immersion periods and each spectrum is characterised by a single full semi-circle. The size of the semicircle in Nyquist plot increases with all increase in time immersion. The calculated values of R_t ($\Omega\text{ cm}^2$) for mild steel immersed in the inhibited H_2SO_4 solution at different exposure times and corresponding inhibition efficiency (E_{Rt} %) are set out in Table 11.

It is seen from Figure 8 that the impedance diagrams do show semi-circles. It is found that the R_t values for steel in 1 M H_2SO_4 with the combined inhibitor (copolymer + KI) increase with immersion time. The obtained impedance diagrams have an almost semi-circular appearance, indicating that a charge transfer process mainly controls the corrosion of mild steel. In fact, the presence of 10 mg/l of copolymer + 0.010 % KI compound enhances the value of R_t in acidic solution.

The change in R_t values and, consequently, of the inhibition efficiency may be due to the gradual replacement of water molecules by the iodide ions and by the adsorption of copolymer molecules on the metal surface, decreasing the extent of dissolution [11, 32] and the results may be due to the adsorption of this compound on the metal surface leading to the formation of film from acidic solution. Some authors attributed this phenomenon to the film formed by the protective molecule inhibitors being thicker when the immersion time increases [49].

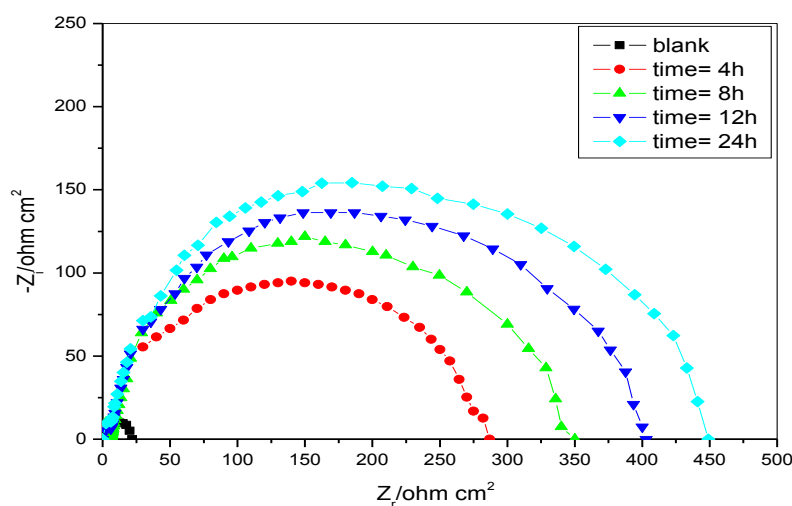


Figure 8. Effect of immersion time on Nyquist plots of mild steel in 1M H_2SO_4 in the presence of (10 mg/l copolymer + 0.010% KI)

Table 11. Effect of immersion time on the inhibition efficiency of (copolymer 10 mg l⁻¹ + KI 0.010%) obtained from impedance measurements

Immersion time (h)	R _i (Ω cm ²)	E(%)
4	287	92.35
8	355	93.80
12	403	94.54
24	449	95.10

3.5 Effect of temperature

The effect of temperature on the inhibited acid–metal reaction is very complex, because many changes occur on the metal surface such as rapid etching, desorption of inhibitor, and the inhibitor itself may undergo decomposition. The change of the corrosion rate at selected concentrations of the copolymer during 2 h of immersion with the temperature was studied in 1 M H₂SO₄, both in absence and presence of 10mg/l of the copolymer alone and with 0.01% KI. For this purpose, gravimetric experiments were performed at different temperatures (291–323 K); the corresponding results are given in Table 12.

The inhibition efficiency (E%) and degree of surface coverage (Θ) of the inhibitor in the presence and absence of KI were calculated using Eqs. (1) and (6) [49, 50].

$$\Theta = \frac{W - W'}{W} \quad (6)$$

Where W and W' are the corrosion rate of steel due to the dissolution in 1M H₂SO₄ in the absence and the presence of definite concentrations of inhibitor, respectively. Θ is the degree of surface coverage of the inhibitor.

Table 12. Various corrosion parameters for mild steel in 1M H₂SO₄ in absence and presence of 10 mg l⁻¹ of the copolymer with and without 0.010% KI at different temperatures

Inhibitor	Temperature(K)	W(mg/cm ² .h)	P%	Θ
Blank	291	0.1686	—	—
	298	0.3329	—	—
	313	2.5665	—	—
	323	6.0103	—	—
Copolymer 10mg.l ⁻¹	291	0.0570	66.2	0.662
	298	0.1168	64.9	0.649
	313	0.8033	68.7	0.687
	323	1.8091	69.9	0.699
Copolymer 10mg.l ⁻¹ + KI 0.010%	291	0.0162	90.4	0.904
	298	0.0359	89.2	0.892
	313	0.1155	95.5	0.955
	323	0.1803	97.0	0.970

From these results, we can deduce that the corrosion rate increases in the blank with the rise of temperature, but in the presence of the copolymer and copolymer with KI, the dissolution of mild steel is widely retarded. The values of inhibition efficiency obtained from the weight loss at various temperatures show that the inhibition efficiency increases with increasing temperature indicating that higher temperature favours the adsorption of copolymer and copolymer with KI on the dissolution of steel at the surface. The corrosion process and protectiveness of an inhibitor are significantly dependent on the temperature.

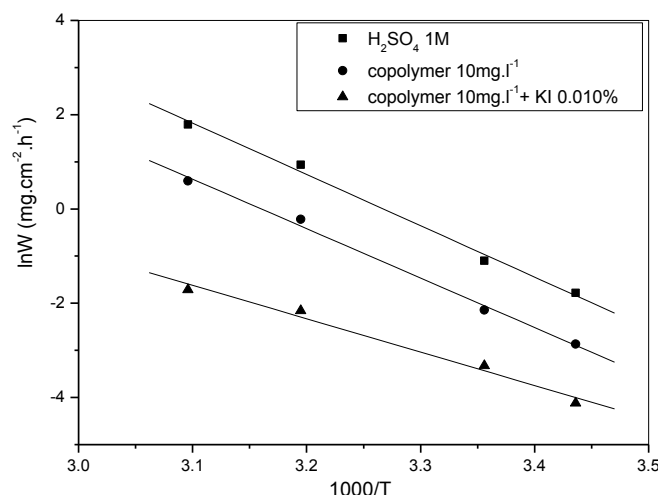


Figure 9. Arrhenius plots for mild steel in 1M H₂SO₄ in the absence and the presence of 10 mg l⁻¹ of the copolymer alone and with 0.010% KI

Figure 9. shows the Arrhenius plots (the logarithm of steel corrosion rate vs. 1000/T) for the corrosion rate for both the blank, inhibitor and inhibitor + KI solution.

From this relation (7), we can determine the apparent activation energies:

$$\ln(W) = \frac{-E_a}{RT} + A \quad \text{and} \quad \ln(W') = \frac{-E'_a}{RT} + A \quad (7)$$

E_a and E'_a are the apparent activation energies with and without the copolymer respectively, T is the absolute temperature, A is a constant and R is universal gas constant.

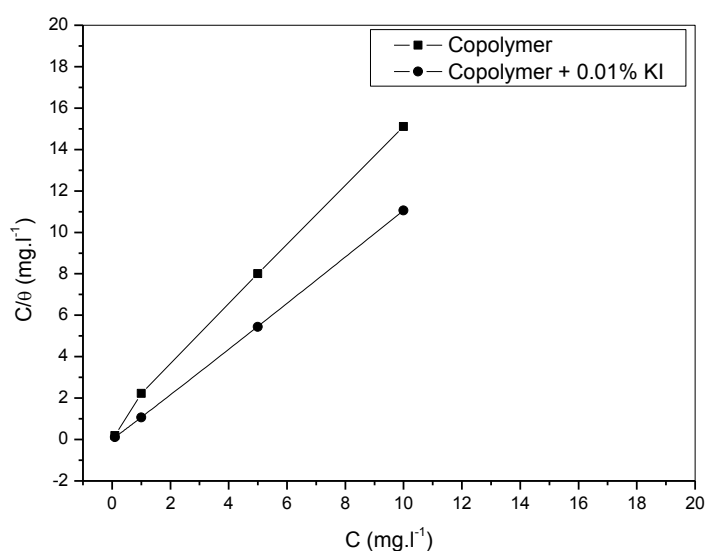
Table 13 present the calculated values of E_a in inhibited and uninhibited acid. It is observed that the activation energy is lower in the presence of copolymer inhibitor than in its absence. The decrease in E_a in inhibited solutions and the previously considered influence of temperature on the protective effect support the assumption for chemisorption of the copolymer and (copolymer + KI) on the metal surface [51, 52]. Szauer et al. [53, 54] state that the lower activation energy value of the process in the presence of the inhibitor compared to that in its absence can be attributed to its chemisorption, while the opposite is the case with physical adsorption.

Table 13. Values of activation energy E_a for mild steel in 1 M H_2SO_4 in absence and presence of additives

Sample	E_a (KJ mol ⁻¹)
H_2SO_4 1M	26.378
Copolymer 10 mg l ⁻¹	24.634
Copolymer + KI 0.01%	17.346

3.6. Adsorption isotherm

Adsorption isotherms are very important for the understanding of the mechanism of organo-electrochemical reaction. The most frequently used isotherms are Langmuir, Frumkin, Temin, Parsons, etc. [7, 15, 17, 21, 46, 48]. The type of the adsorption isotherms provides information about the interaction among the adsorbed molecules them selvesand also their interactions with the electrode surface.

**Figure 10.** Langmuir adsorption isotherm of the copolymer and (copolymer + KI) on the mild steel surface in 1 M H_2SO_4 from loss measurements.

The adsorption of the organic compounds can be described by two main types of interaction: physical adsorption and chemisorption. These are influenced by the chemical structure of the inhibitor, the type of the electrolyte and the charge and nature of the metal. The surface coverage Θ of the metal surface by the adsorbed inhibitor was calculated using the Eq. (6):

The θ values for different inhibitor concentrations at different temperatures were tested by fitting to various isotherms. Several adsorption isotherms were assessed and the Langmuir adsorption isotherm was found to be the best description of the adsorption behavior of the studied inhibitor. According to this isotherm Θ is related to concentration inhibitor C via

$$\frac{C}{\Theta} = \frac{1}{K} + C \quad (8)$$

where K designates the adsorption equilibrium constant. This equation is the ideal equation that should be applied to the ideal case of the physical and chemical adsorption on a smooth surface with no interaction between adsorbed molecules. It was found that a plot of C/Θ vs C gives straight lines, showing that the adsorption of the copolymer alone and in combination with KI from H_2SO_4 1 M on the mild steel surface obeys the Langmuir adsorption isotherm (Figure 10)

4. Conclusions

- The poly(acrylamide-co-4-vinylpyridine) copolymer inhibits the corrosion of mild steel in H_2SO_4 and affects both anodic and cathodic Tafel slopes.
- Synergistic effects between the poly(acrylamide-co-4-vinylpyridine) copolymer and KI have been observed. The addition of KI significantly enhances the inhibition efficiency of the copolymer. The adsorption of the copolymer is stabilized by the presence of iodide ions in the solutions.
- The inhibition efficiency found from weight loss, polarization curves, electrochemical impedance spectroscopy measurements are in good agreement.
- The inhibition efficiency of (copolymer + KI) improves with increasing immersion time.
- The chemisorption of the copolymer is stabilized by the presence of iodide ions in the solutions.
- The adsorption of the copolymer and (copolymer + KI) on the metal surface from 1 M H_2SO_4 obeys the Langmuir adsorption isotherm model.

References

- [1] H. Bhandari, V. Choudhary, S. K. Dhawan, *Synth. Met*, 161 (2011) 753.
- [2] I. Elouali, B. Hammouti, A. Aouniti, Y. Ramli, M. Azougagh, E. M. Essassi, M. Bouachrine, *J. Mater. Environ. Sci*, 1 (2010) 1.
- [3] M. B. Nemer, Y. L. Xiong, A. E. Ismail, J.H. Jang, *Chem. Geol*, 280 (2011) 26.
- [4] J. Soltis, D. Krouse, N. Laycock, *Corros. Sci*, 53 (2011) 2152.
- [5] S. A. Umoren, Y. Li, F. H. Wang, *Corros. Sci*, 53 (2011) 1778.
- [6] A. Chetouani, M. Daoudi, B. Hammouti, T. Ben Hadda, M. Benkaddour, *Corros. Sci*, 48 (2006) 2987.
- [7] A. Chetouani, K. Medjahed, K. E. Sid-Lakhdar, B. Hammouti, M. Benkaddour, A. Mansri, *Corros. Sci*, 46 (2004) 2421.
- [8] O. K. Abiola, M. O. John, P. O. Asekunowo, P. C. Okafor, O. O. James, *Green Chem. Lett. Rev*, 4 (2011) 273.
- [9] D. Bankiewicz, E. Alonso-Herranz, P. Yrjas, T. Lauren, H. Spliethoff, M. Hupa, *Energy Fuels*, 25 (2011) 3476.

- [10] M. Behpour, S. M. Ghoreishi, N. Mohammadi, M. Salavati-Niasari, *Corros. Sci.*, 53 (2011) 3380.
- [11] F. Bentiss, M. Traisnel, M. Lagrenee, *Corros. Sci.*, 42 (2000) 127.
- [12] X. L. Cheng, H. Y. Ma, S. H. Chen, R. Yu, X. Chen, Z. M. Yao, *Corros. Sci.*, 41 (1999) 321.
- [13] M. Ajmal, J. Rawat, M. A. Quraishi, *Br. Corros. J.*, 34 (1999) 220.
- [14] S. A. Abd El-Maksound, *Int. J. Electrochem. Sci.*, 3 (2008) 528.
- [15] A. Chetouani, B. Hammouti, A. T. Benhadda, M. Daoudi, *Appl. Surf. Sci.*, 249 (2005) 375.
- [16] A. Chetouani, B. Hammouti, *Bull. Electrochem.*, 20 (2004) 343.
- [17] A. Chetouani, A. Aouniti, B. Hammouti, N. Benchat, T. Benhadda, S. Kertit, *Corros. Sci.*, 45 (2003) 1675.
- [18] A. Chetouani, B. Hammouti, *Bull. Electrochem.*, 19 (2003) 23.
- [19] K. Laarej, M. Bouachrine, S. Radi, S. Kertit, B. Hammouti, *J. Chem.*, 7 (2010) 419.
- [20] K. Barouni, L. Bazzi, R. Salghi, M. Mihit, B. Hammouti, A. Albourine, S. El Issami, *Mater. Lett.*, 62 (2008) 3325.
- [21] A. Ouchrif, M. Zegmout, B. Hammouti, A. Dafali, M. Benkaddour, A. Ramdani, S. Elkadiri, *Prog. Org. Coat.*, 53 (2005) 292.
- [22] M. Zerfaoui, H. Oudda, B. Hammouti, S. Kertit, M. Benkaddour, *Prog. Org. Coat.*, 51 (2004) 134.
- [23] M. A. Amin, K. F. Khaled, Q. Mohsen, H. A. Arida, *Corros. Sci.*, 52 (2010) 1684.
- [24] N. Bertrand, C. Desgranges, D. Poquillon, M. C. Lafont, D. Monceau, *Oxid. Met.*, 73 (2010) 139.
- [25] C. Jeyaprabha, S. Sathiyarayanan, G. Venkatachari, *Appl. Surf. Sci.*, 253 (2007) 432.
- [26] S. A. Umoren, E. E. Ebenso, *Mater. Chem. Phys.*, 106 (2007) 387.
- [27] S. A. Umoren, Y. Lia, F. H. Wang, *Corros. Sci.*, 52 (2010) 1777.
- [28] S. A. Umoren, Y. Lia, F. H. Wang, *Corros. Sci.*, 52 (2010) 2422.
- [29] Y. Abed, B. Hammouti, F. Touhami, A. Aouniti, S. Kertit, A. Mansri, K. Elkacemi, *Bull. Electro-chem.*, 17 (2001) 105.
- [30] A. Chetouani, K. Medjahed, K. E. Benabadji, B. Hammouti, S. Kertit, A. Mansri, *Prog. Org. Coat.*, 46 (2003) 312.
- [31] Y. Abed, Z. Arrar, B. Hammouti, F. Touhami, M. Taleb, S. Kertit, A. Mansri, *Anticorros. Methods Mater.*, 48 (2001) 304.
- [32] L. Larabi, Y. Harek, M. Traisnel, A. Mansri, *J. Appl. Electrochem.*, 34 (2004) 833.
- [33] L. Larabi, Y. Harek, *Portgu. Electrochim. Acta*, 22 (2004) 227.
- [34] S. A. Umoren, O. Ogbobe, E. E. Ebenso, U. J. Ekpe, *Pigmen Resin Technol.*, 35 (2006) 284.
- [35] S. A. Umoren, U. M. Eduok, E. E. Oguzie, *Portgu. Electrochim. Acta*, 26 (2008) 533.
- [36] S. A. Umoren, O. Ogbobe, E. E. Ebenso, *Bull. Electrochem.*, 22 (2006) 155.

- [37] A. Mansri, B. Bouras, B. Hammouti, I. Warad, A. Chetouani, Res Chem Intermed 10.1007/s11164-012-0547-4 (2012)
- [38] B. Grassl, G. Clisson, A. Khoukh, L. Billon, Eur. Polym. J, 44 (2008) 50.
- [39] Z. Gui, J. Qian, Q. An, H. Xu, Q. Zhao, Eur Polym. J, 45 (2009) 1403.
- [40] S. Belkaid, K. Tebbji, A. Mansri, A. Chetouani, Res Chem Intermed 10.1007/s11164-012-0547-4 (2012)
- [41] K. Benmansour, K. Medjahed, L. Tennouga, A. Mansri, Eur. Polym. J, 39 (2003) 1443.
- [42] Y. Bernard, D. Coleman, R. M. Fuoss, J. Am. Chem. Soc, 77 (1955) 5472.
- [43] K. L. Khaled, Electrochim. Acta, 48 (2003) 2493.
- [44] F. Bentiss, M. Lagrennee, M. Traisnel, J. C. Hornez, Corros. Sci, 41 (1999) 789.
- [45] G. Mu, X. Li, Q. Qu, J. Zhou, Corros. Sci, 48 (2006) 445.
- [46] M. Bouklah, A. Attayibat, S. Kertit, A. Ramdani, B. Hammouti, Appl. Surf. Sci, 242 (2005) 399.
- [47] C. Jeyaprabha, S. Sathiyarayanan, S. Muralidharan, G. Venkatachari, J. Braz. Chem. Soc, 17 (2006) 61.
- [48] A. Chetouani, B. Hammouti, A. Aouniti, N. Benchat, T. Benhadda, Prog. Org. Coat, 45 (2002) 373.
- [49] S. R. Lodha, Pharm. Rev, 6 (2008) 1.
- [50] A. Zarrouk, B. Hammouti, H. Zarrok, I. Warad, M. Bouachrine, Der Pharma Chem, 2 (2011) 263.
- [51] F. S. de Souza, A. Spinelli, Corros. Sci, 51 (2009) 642.
- [52] C. Selles, O. Benali, B. Tabti, L. Larabi, Y. Harek, J. Mater. Environ. Sci, 3 (2012) 2028.
- [53] T. Szauer, A. Brandt, Electrochim. Acta, 26 (1981) 1209.
- [54] Z. A. Foroulis, in Proceedings of the 6th European Symposium on Corrosion Inhibitors, Ferrara, 48 (1985).